Life Sciences 220 (2019) 8–20

Contents lists available at ScienceDirect

Life Sciences

journal homepage: www.elsevier.com/locate/lifescie

Niclosamide alleviates pulmonary fibrosis *in vitro* and *in vivo* by attenuation of epithelial-to-mesenchymal transition, matrix proteins & Wnt/β-catenin signaling: A drug repurposing study

Raju Boyapally[1], Gauthami Pulivendala[1], Swarna Bale, Chandraiah Godugu[*]

Department of Regulatory Toxicology, National Institute of Pharmaceutical Education and Research (NIPER), Balanagar, Hyderabad, Telangana, 500037, India

ARTICLE INFO

Keywords:
Niclosamide
Pulmonary fibrosis
EMT
Wnt/β-catenin

ABSTRACT

Drug repurposing off late has been emerging as an inspiring alternative approach to conventional, exhaustive and arduous process of drug discovery. It is a process of identifying new therapeutic values for a drug already established for the treatment of a certain condition. Our current study is aimed at repurposing the old anti-helimenthic drug Niclosamide as an anti-fibrotic drug against pulmonary fibrosis (PF). PF is most common lethal interstitial lung disease hallmarked by deposition of extracelluar matrix and scarring of lung. Heterogenous nature, untimely diagnosis and lack of appropriate treatment options make PF an inexorable lung disorder. Prevailing void in PF treatment and drug repositioning strategy of drugs kindled our interest to demonstrate the anti-fibrotic activity of Niclosamide. Our study is aimed at investigating the anti-fibrotic potential of Niclosamide in TGF-β1 induced *in vitro* model of PF and 21-day model of Bleomycin induced PF *in vivo* respectively. Our study results showed that Niclosamide holds the potential to exert anti-fibrotic effect by hampering fibroblast migration, attenuating EMT, inhibiting fibrotic signaling and by regulating WNT/β-catenin signaling as evident from protein expression studies. Our study findings can give new directions to development of Niclosamide as an anti-fibrotic agent for treatment of pulmonary fibrosis.

1. Introduction

Drug repositioning, otherwise referred as therapeutic switching is historically pragmatic in accelerating drug development and assists as a cost effective approach to treat unmet medical needs [1,2]. It implicates a unique feature of identifying a new medical indication for known drugs, thereby significantly reducing cost, time and risk involved in the process of drug development [3,4]. This process of drug repositioning includes an approach of computational biology along with several *in vitro* and *in vivo* experimental studies to accomplish the proposed hypothesis for existing drugs to treat different diseases [5]. Furthermore, in the era of omics with the help of emerging tools, drug repositioning is now explored as an opportunity that utilizes tailored and personalized approaches. Contribution of drug repositioning in rare disease areas like pulmonary fibrosis therefore gains huge significance owing to the scope of interplay between the specific disease and existing drugs. Recent evidences demonstrate that several drug repurposing studies in the past were published on identifying potential therapeutic targets against Alzheimer's, malaria, tuberculosis, and various cancers using *in silico* studies [6–9]. Very recently, *in silico* repurposing studies against pulmonary fibrosis for the first time was performed in *in-vitro* and *in-vivo* experiments and obtained promising results using various drugs [10,11].

PF is a rare, untreatable condition among various interstitial lung diseases, manifested by myofibroblasts activation. The key concept behind fibrosis research involves its complex pathophysiology thereby focusing on such a complex fibrotic process can improve the flexibility of identifying a better therapeutic compound [12]. Multiple signaling Smad dependent and independent pathways are critical in the pathogenesis of PF [13] of which Wnt/β-catenin pathway gains significance as an emerging target owing to its activation in the progression of PF; might be a promising target in combating PF [14,15]. Lung architecture is devastated resulting in exacerbated epithelial to mesenchymal transition (EMT) and extracellular matrix (ECM) deposition inculpated by

[*] Corresponding author at: Department of Regulatory Toxicology, NIPER-Hyderabad, India.
E-mail address: chandragodugu@gmail.com (C. Godugu).
[1] Equal contribution.

https://doi.org/10.1016/j.lfs.2018.12.061
Received 17 September 2018; Received in revised form 31 December 2018; Accepted 31 December 2018
Available online 03 January 2019
0024-3205/

factors damaging the alveolar epithelium [16]. The distorted epithelium aids in enhanced fibroblast recruitment, their proliferation and differentiation sequenced by cellular and signaling events contributing to irreversible fibrosis of the lung tissue [17]. It is therefore essential to develop adequate therapeutic drugs that impede PF.

Niclosamide (NCL), an oral antihelminthic drug approved by US FDA is used to treat various infections of intestinal cestodes for > 50 years due to its potential of inhibiting mitochondrial oxidative phosphorylation. Significant findings from the literature demonstrate the effect of NCL in various solid cancers by regulating multiple signaling pathways including Notch-signaling, ERK, STAT 3 and Wnt/β-catenin pathway and by inhibiting several key inflammatory cytokines [18,19]. Further, this multiple pathway inhibitor is found to play a central role in ameliorating TGF-β1 induced profibrotic effects in some of the fibrotic diseases including renal and skin fibrosis [20,21]. Moreover, computational biological studies predicted NCL to exhibit strong anti-fibrotic effects in attenuating PF [10]. Besides, NCL is known as potent inhibitor of Wnt/β-catenin signaling and given the significance of Wnt/β-catenin signaling in PF [22,23], the present study aims at investigating the anti-fibrotic potential of NCL in well established TGF-β1 induced *in vitro* and Bleomycin (BLM) induced *in vivo* experimental models.

2. Material & methods

2.1. Chemicals

Niclosamide was purchased from Sigma-Aldrich; USA, Bleomycin sulfate was obtained from Cipla labs; India, Human recombinant TGF-β1 was obtained from Biolegend USA, Trans-L-Hydroxyproline, Chloramine-T, Bicinchoninic acid, Ehrlich reagent, RIPA lysis buffer, Direct red, Picric acid, Griess reagent, Bradford reagent, Sodium nitrite, Bovine serum albumin (BSA), and Sodium dodecyl sulphate (SDS) were procured from Sigma-Aldrich; USA. T-PER was procured from Thermo Fisher Scientific; USA. Enzyme linked immunosorbent assay (ELISA) kits were procured from eBiosciences; USA. Anti-β-Actin, anti-α-SMA, anti-E-cadherin, anti-fibronectin, anti-CTGF, anti-TGF-β1 antibodies were purchased from Santa Cruz Biotechnology; USA and anti-p PDGF-BB, anti-PDGF-BB, anti-Smad2/3, anti-p Smad2/3, anti-survivin, anti-MET, anti-β-catenin, anti-CD44, anti-c-Myc, c-Jun, anti-GSK3β, anti-WNT, anti-LEF, anti-NF-κβ and anti-pNF-κβ antibodies were purchased from Cell Signaling technology; USA. All other chemicals and reagents used for this study were of analytical grade and procured commercially.

2.2. Cell culture

Human fetal lung fibroblasts (HFL1) cells were purchased from ATCC (ATCC® CCL153™), supplemented with anti-biotic solution (1%) and fetal bovine serum (10%) cultured in Kaighn's modification of Ham's F-12 Medium (F-12 K); Invitrogen, USA. TGF-β1 stimulation at a concentration of 10 ng/mL was used to induce fibrotic events. NCL was made as stock concentration of 10 mM using DMSO as solvent, stored at −20 °C and diluted as per the working concentrations before use. Cultured cells maintained at 37 °C in 5% CO2 incubator were treated with NCL at concentrations of 30 and 100 nM with and without TGF-β1 stimulation and incubated for 24 h, harvested and used for further experiments.

2.3. Cytotoxicity assay using MTT

Cell viability of NCL on HFL1 cells was investigated using MTT assay (3-(4, 5-dimethylthiazol-2-yl)-2, 5-diphenyltetrazolium bromide). HFL1 cells at a density of 10^3 cells per well were seeded in a 96 well plate and after 24 h of seeding, cells were treated with NCL. Media from the plate was discarded and fresh media containing MTT solution (100 μL per each well of 5 mg/10 mL concentration) was added to cells after 24 h of incubation with NCL and incubated further for 4 h with DMSO (200 μL/well) to dissolve the formed formazan crystals. After 20 min of DMSO incubation, the absorbance of the cells was measured using a multi-mode spectrophotometer at a wavelength of 570 nm. IC_{50} was derived from concentration *vs*. absorbance curve (concentration of NCL *vs*. absorbance of DMSO solubilized formazan crystals) [24].

2.4. Scratch wound assay

Scratch wound assay was performed to evaluate the potential of NCL on cell migration. In brief, HFL1 cells with density of 10^5 cells were seeded in a 12 well culture plate and when cells attained 70–80% of confluence, a gap in a straight line of mono adherent cells was made using a 10 μL micropipette tip, cells were washed with PBS twice so as to remove the detached cells while creating a gap. Later cells were treated with TGF-β1 alone and NCL in the presence and absence of TGF-β1 growth factor for 24 h. Images of the cells with gap in all groups were captured initially at 0 h and after 24 h of treatment, followed by measuring the width of the gap using microscopic scaling and graph pad prism software was used to quantify the measured width [25].

2.5. Animals and grouping

Eight week old male Swiss albino mice obtained from Palamur Biosciences private limited (Mahabubnagar, India), were allowed to acclimatize for a week. All animals were allowed free access to food and water ad libitium, and maintained with 12/12 h light and dark conditions. Animal experimental protocols were duly approved by institutional animal ethics committee (IAEC) of NIPER-Hyderabad and *in vivo* studies were performed with relevant guidelines. Animals were randomly assigned into following groups (n = 10): Control group; BLM alone group (1.5 IU/kg); BLM + NCL low dose (3 mg/kg); BLM + NCL high dose (10 mg/kg) and Perse (NCL alone group), 10 mg/kg. DMSO and polyethylene glycol 200 (1:4 ratio) in normal saline was used as vehicle for administration of NCL. The concentration of DMSO used was 1% in saline. Required amount of NCL was weighed and solubilized in DMSO:PEG (1:4 ratio) in saline, then probe sonicated thoroughly before administration. Mice were administered intratracheally with 1.5 IU/Kg of BLM on day 0 while NCL was administered daily once from day 1 to day 21 by intraperitoneal (i.p) route. On the day of termination (day 21), lungs were harvested, stored and used for estimating various biochemical parameters, pathological and molecular studies.

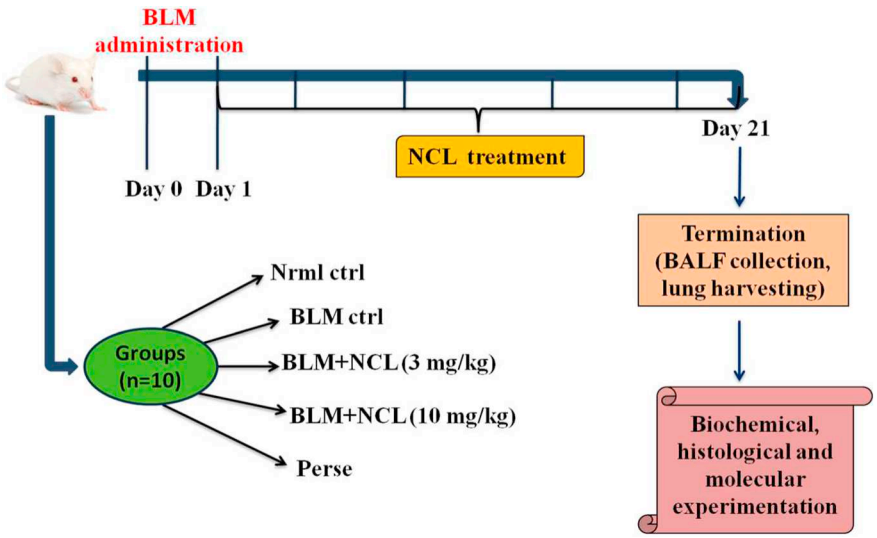

Diagrammatic representation of study design and experimental groups used in the study.

2.6. Lung bronchoalveolar lavage fluid (BALF) biochemical parameters

BALF, a reliable parameter to assess lung fibrosis was gently aspirated from trachea of the mice by inserting a suitable catheter using ice cold PBS of 1 mL passing each time thrice. BALF thus collected was pooled and subjected to evaluate differential cell count by automatic Siemens hematology system (model-Advia 2120i).

2.7. Lung tissue biochemical parameters

2.7.1. Griess assay to estimate nitric oxide (NO) levels

Lung tissues were homogenized and centrifuged at 10,000 rpm maintained at 4 °C and supernatants were collected and used immediately to measure NO levels. Griess reagent was used to evaluate the NO levels of the samples by mixing equal proportions of both Griess reagent and supernatants of lung tissue samples, incubated for 10 min in dark conditions, and absorbance was measured at 548 nm. Data obtained from the experiments was normalized using protein content and expressed as μM/mg of lung protein. Sodium nitrite was used as calibrator [26].

2.7.2. Hydroxyproline assay to determine collagen levels

Hydroxyproline content in the lung tissue homogenates was estimated as per protocol performed by Bale et al. [27]. Lung tissues were homogenized at 4000 rpm and subjected to acid hydrolysis (6 N HCl). Later, Chloramine-T was added to hydrolyzed homogenates to undergo oxidation and incubated for 15 min. To the obtained oxidized samples, Ehrlich reagent was added and incubated further at 60 °C for 20 min. The samples were allowed to cool and absorbance was read at 550 nm. Hydroxyproline was used as standard and accordingly, concentrations of samples were measured from concentration-absorbance curve. Values were normalized using lung protein content obtained by Bradford assay.

2.7.3. Sircol assay for collagen estimation

Collagen binding dye was added to the lung supernatants and incubated at 37 °C for 1 h. Samples were then centrifuged, supernatant was discarded and visibly obtained red pellet was dissolved in absolute alcohol to remove the accumulated binding dye and further centrifuged. The pellet formed was dissolved in alkali solution (0.5 M sodium chloride) and incubated at 37 °C for 30 min. Following incubation of the samples, absorbance was measured using multimode spectrophotometer at 540 nm. Data obtained was normalized with lung protein content estimated by Bradford assay [25].

2.7.4. ELISA for estimation of inflammatory cytokines

Lung tissues were thoroughly homogenized using ELISA extraction buffer and centrifuged at 4 °C; supernatants obtained were stored at −80 °C as aliquots. Various pro-inflammatory cytokines including IL-6, IL-1β and TNF-α were estimated for their expression in extracted tissue supernatants using a commercially available ELISA kit based method. The procedure for estimating the above mentioned cytokines were followed as per the manufacturers' instructions. Cytokine expression of all the samples was normalized with protein content of the respective supernatants obtained using Bradford assay, and results were expressed as pg/mg of protein obtained from the plot of concentration-absorbance curve of standards supplied along with the kit.

2.8. Pathological studies

Left lobes of the lung tissue harvested on the day of termination were fixed in non buffered formalin solution (10%). After 2 days of fixation, tissues were processed and embedded in paraffin. Later, the embedded blocks were made into 5 μ thick sections and stored at 37 °C overnight. These sections were then subjected to haematoxylin and eosin staining to visualize the altered pathological changes. Similarly, Sirius red staining and toluidine blue staining were performed with the lung tissue sections so as to investigate the extent of collagen and mast cell accumulation respectively. The procedure for these staining techniques was performed as per established standard protocols.

2.9. Immunohistochemistry

5 μ thick sections of lung tissue were deparaffinised in xylene followed by subjecting to rehydration using a series of gradient alcohols (100, 90, 80 and 70%) for an interval of 3 min each. Later, tissue sections were processed for antigen retrieval using proteinase K solution at a concentration of 20 μg/mL prepared in tris buffer adjusted to pH 8, followed by treatment with 3% H_2O_2 to eliminate endogenous peroxidase. Subsequently, to avoid nonspecific binding, sections were treated with 3% BSA blocking solution for 1 h, washed twice with PBST (phosphate buffered saline-tween 20) and incubated with primary antibodies (rabbit anti-β-catenin and mouse anti-fibronectin at dilutions of 1:100 in 3% BSA blocking solution) for overnight at 4 °C. The next day, sections were effectively washed with PBST and underwent to develop colour by exposing to poly Excel HRP/DAB Detection System (PathnSitu Biotechnologies Pvt. Ltd., Hyderabad, India); counterstained with haematoxylin and mounted with DPX resinous solution. The mounted lung sections were visualized for immunopositivity and

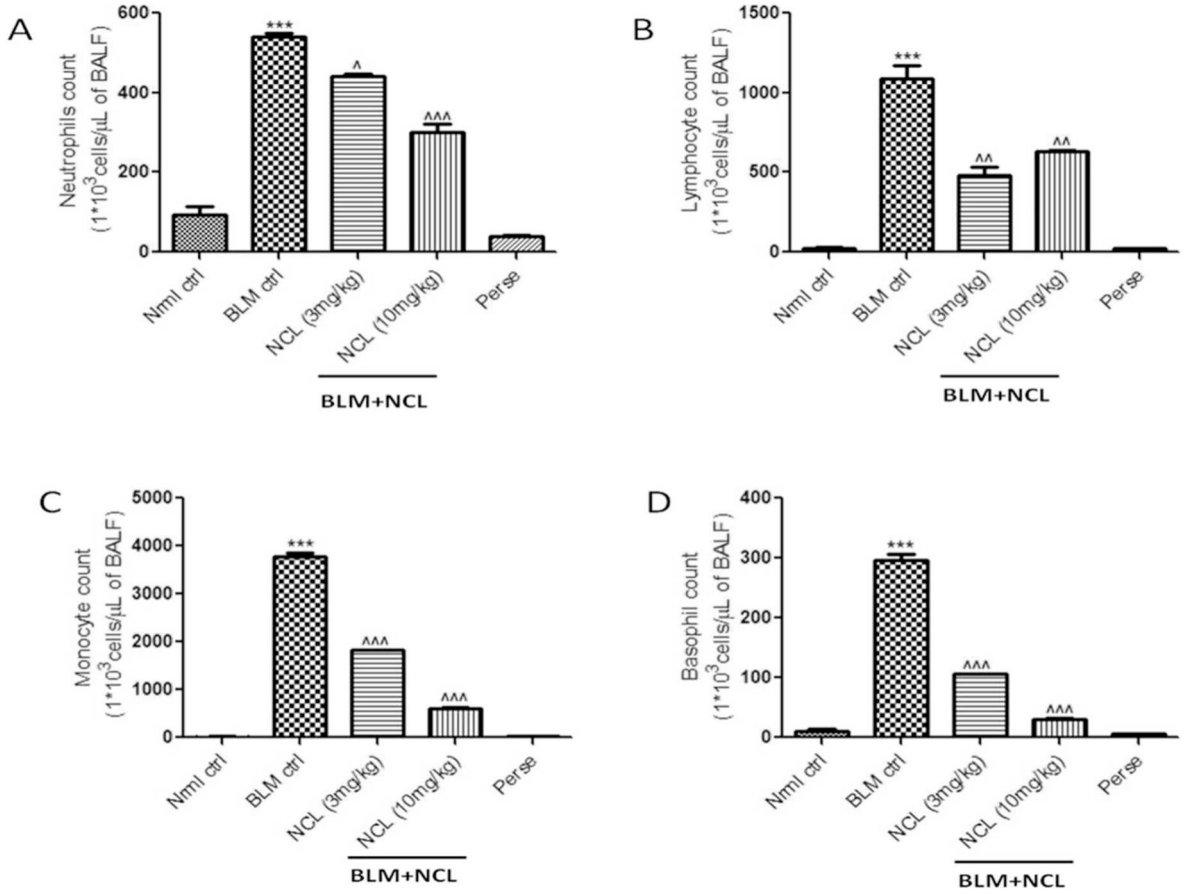

Fig. 1. Effect of NCL on differential count of inflammatory cell infiltrates in BALF collected from lung on day of termination (day 21). (A) Neutrophils (B) Lymphocytes (C) Monocytes (D) Basophils. BALF collected from NCL treated mice demonstrated significantly reduced differential counts of inflammatory cells as compared to that of BALF from BLM treated mice. Data expressed as mean ± SEM, ***$p < 0.001$ of BLM *vs*. Nrml ctrl; ^^^$p < 0.001$, ^^$p < 0.01$ and ^$p < 0.5$ of NCL *vs*. BLM.

images were captured using Olympus microscope [25].

2.10. Western blotting

In vitro HFL1 cells were lysed using radio immunoprecipitation assay buffer (RIPA), while *in vivo* lung tissues were processed for homogenization using tissue protein extraction reagent (T-PER). Bicinchoninic acid was used to determine the protein concentration in the obtained supernatants, followed by protein separation on SDS polyacrylamide gels and transferred onto nitrocellulose/polyvinyldifluoride membranes. Proteins of interest that were transferred on the membranes were washed effectively using TBST and allowed to incubate with 3% BSA for 90 min to eliminate non-specific binding. After incubation, blots were washed twice with TBST and further incubated with primary antibody maintained at 4 °C for overnight. The following day, antibody was recovered and blots were washed with TBST for three times with an interval of 10 min; allowed to react with respective secondary antibody for 2 h at room temperature, washed 3–4 times using TBST before visualizing the protein expression using chemi imaging detection system (Vilber Fusion Fx); France. The obtained immunoblots were quantified using Image J software. β-actin is used as a house keeping protein for normalization [28].

2.11. Statistical analysis

All results in the study were expressed as mean ± SEM of three independent experiments. Statistical analysis of the obtained was performed by one-way ANOVA followed by Tukey's *post hoc* test. All statistical analyses were performed using v.5 GraphPad Prism software. *P* value < 0.05 levels were considered as statistically significant.

3. Results

3.1. Effect of NCL on BALF differential cell count

BAL fluid collected on the day of termination was analyzed for differential counts *i.e.*; neutrophils, lymphocytes, basophils and monocytes counts. Intratracheal instillation of BLM caused significant elevation in neutrophils, lymphocytes, basophils and monocytes counts in the BAL fluid as compared to BAL fluid obtained from mice of normal control. Daily administration of NCL significantly lowered the differential counts in a dose dependent manner (Fig. 1).

3.2. NCL inhibits cell proliferation, migration and modulates proteins involved in EMT both in vitro and in vivo

Initially, we evaluated the effect of NCL on viability of HFL1 cells by performing MTT assay. IC_{50} value of NCL upon 24 h treatment on HFL1 cells was found to be 409.79 ± 0.17 nM from the results of MTT assay. Therefore, for all further *in vitro* experimentations, to elucidate the fibrotic events submaximal concentrations of NCL (30 and 100 nM) were selected. As ability of fibroblasts to migrate is characteristic feature acquired through transition of cell from its epithelial stage to mesenchymal state, we subsequently evaluated the ability of NCL to inhibit cell proliferation and migration of fibroblasts (HFL1) through the standard cell migration assay otherwise known as scratch wound assay

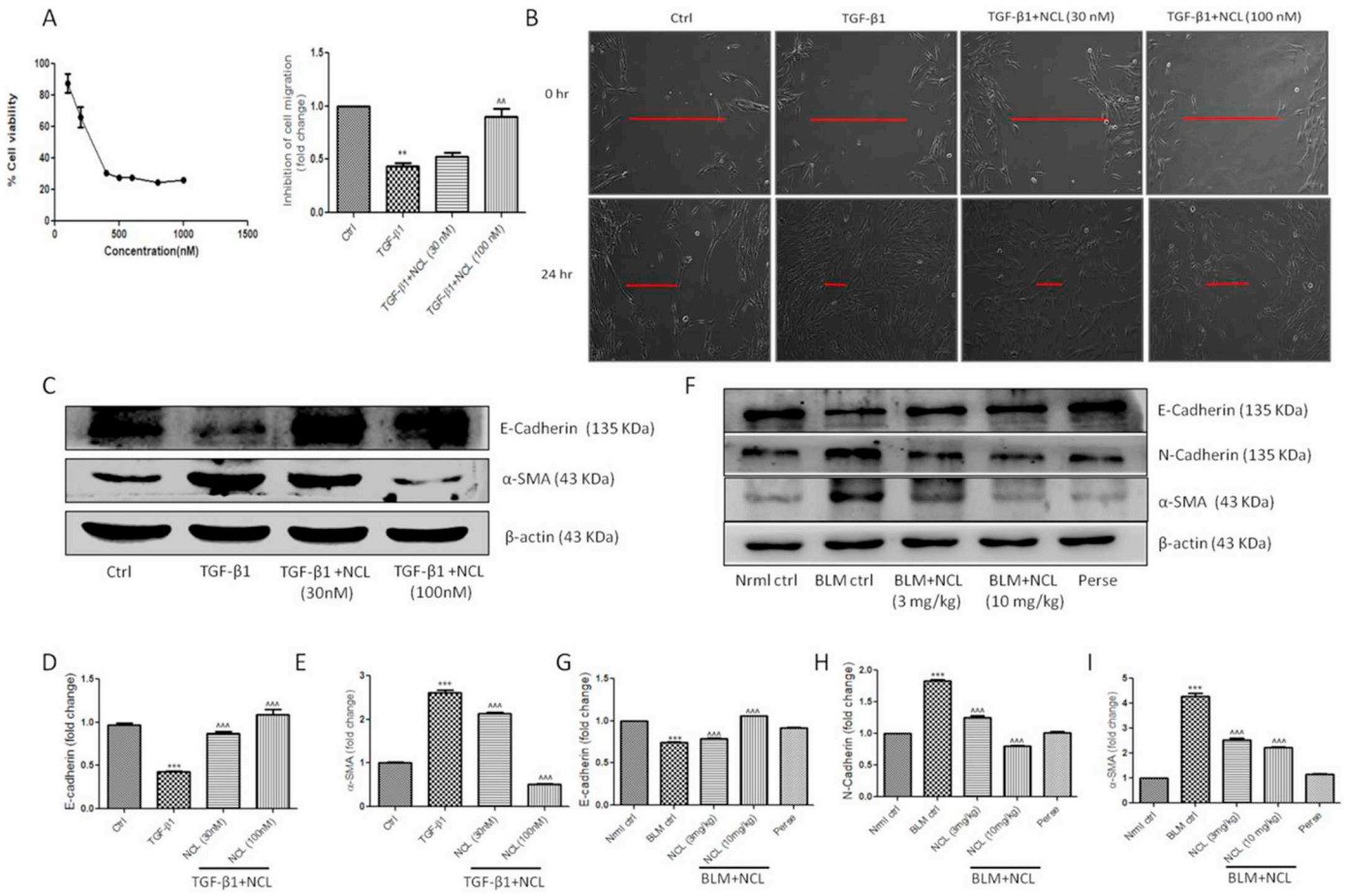

Fig. 2. NCL inhibits cell proliferation, fibroblast migration and EMT markers both *in vitro* and *in vivo*. (A) Effect of NCL on cell viability of HFL1 cells (B) Effect of NCL on fibroblast migration (scratch wound assay) (C) Representative immunoblots of E-cadherin and α-SMA in HFL1 cell lysates (D & E) Graphical representation of quantified protein expression of E-cadherin and α-SMA in HFL1 cell lysates. (F) Western blotting analysis of E-cadherin, N-cadherin and α-SMA in lung tissue lysates (G-I) Densitometric analysis of quantified protein expression of E-cadherin, N-cadherin and α-SMA. Data expressed as mean ± SEM, $^{***}p < 0.001$ and $^{**}p < 0.01$ of disease *vs*. Nrml ctrl and $^{\hat{}\hat{}\hat{}}p < 0.001$ and $^{\hat{}\hat{}}p < 0.01$ of NCL *vs*. disease.

at the above mentioned concentrations. As shown in Fig. 2, TGF-β1 stimulated fibroblasts covered the scratch at the end of 24 h of treatment depicting its high rate of proliferation and migration as compared to unstimulated normal fibroblasts. In contrast, fibroblasts treated with NCL showed a dose dependent reduction in cell proliferation and motility. Therefore, the artificially created scratch in the cell monolayer was partially occupied by fibroblasts at 30 nM, whereas the scratch was very sparsely covered by fibroblasts at 100 nM upon 24 h of NCL treatment.

Post confirming the inhibitory effect of NCL on cell migration, we further investigated the effects of NCL on EMT proteins through western blotting. A notable increase in expression levels of α-smooth muscle actin (α-SMA), a mesenchymal protein, was observed in TGF-β1 treated cells. Upon treatment with NCL, expression of α-SMA was decreased in dose dependent manner. Next, we assessed the expression of E-cadherin, a cell adhesion epithelial marker. As presumed, TGF-β1 stimulated cells represented subsided levels of E-cadherin where as NCL treatment dose dependently restored its levels.

In view of the results obtained with respect to EMT inhibition *in vitro*, expression of EMT proteins was evaluated in lung tissue homogenates *in vivo* through immunoblotting. Similar to the results of *in vitro,* a decrease in epithelial marker E-cadherin was observed following which a corresponding sharp rise in expression levels of N-cadherin was noted in BLM alone treated mice. Additionally, there was significant increase in levels of α-SMA in animals instilled with BLM. NCL treatment not only restored the levels of E-cadherin but also down regulated the expression of N-cadherin and α-SMA significantly. From the consistent results of *in vitro* and *in vivo,* it can be said that NCL exhibits a property of EMT inhibition (Fig. 2).

3.3. NCL down regulates expression of fibrotic proteins induced by TGF-β1 in vitro and BLM in vivo

Consequently, we proceeded to investigate NCL effects on fibrotic proteins involved in TGF-β/Smad signaling. Western blotting of whole cell lysates of TGF-β1 induced HFL 1 cells showed over expression of major fibrotic markers fibronectin, connective tissue growth factor (CTGF), TGF-β1 and phosphorylated Smad when compared to unstimulated cells. NCL down regulated the expression of fibronectin, CTGF, TGF-β1 and phosphorylated Smad significantly in dose dependent manner. Additionally, we observed high expression of p-PDGF-BB receptor in TGF-β1 stimulated HFL1 cells as evident from the immunoblotting. Treatment with NCL significantly reduced the expression of phosphorylated PDGF-BB receptor dose dependently (Fig. 3).

Parallel results were noted upon western blot analysis of lung tissue homogenates. BLM insulted mice displayed an elevated expression of major fibrotic proteins fibronectin, CTGF and TGF-β1 as compared to normal control mice. Daily administration of NCL significantly reduced fibronectin, CTGF and TGF-β1 expression in NCL treated mice at both the doses. Next, immunohistochemical analysis was performed to evaluate the expression levels of fibronectin. Consistent with the results of western blot analysis of fibronectin, BLM treated lung section showed

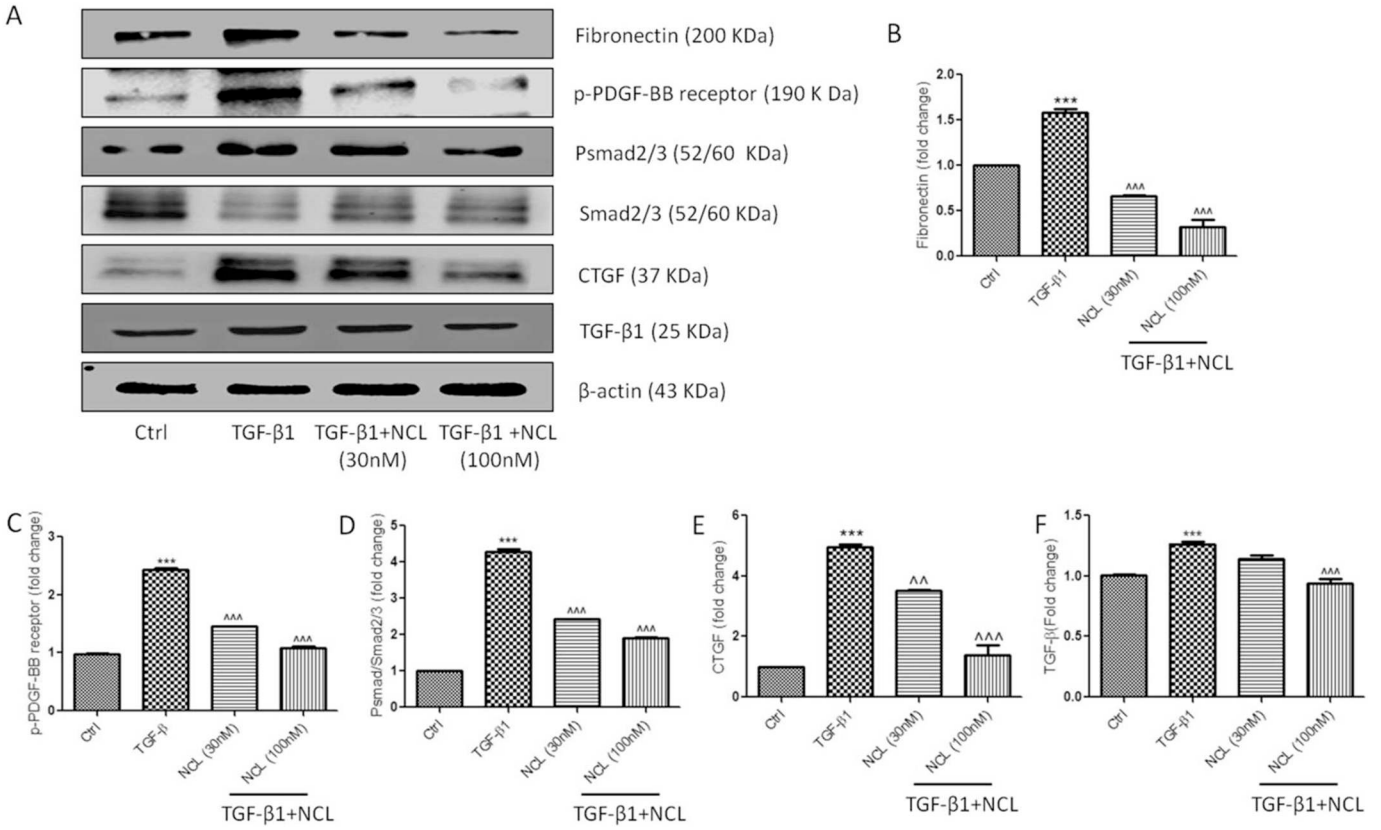

Fig. 3. NCL significantly attenuates TGF-β/Smad signaling and down regulates expression of fibrotic markers *in vitro*. (A) Effect of NCL intervention on fibrotic markers inTGF-β1 stimulated HFL1 cells. Graphical representation of quantified protein expression of (B) Fibronectin (C) p PDGF-BB receptor (D) pSmad/Smad2/3 (E) CTGF and (F) TGF-β1. β-actin was used as internal standard for all the proteins while pSmad was normalized with total protein Smad2/3. Data expressed as mean ± SEM ***$p < 0.001$of TGF-β1 *vs*. Nrml ctrl; ^^^p < 0.001 and ^^$p < 0.01$ of NCL *vs*. TGF-β1.

uniformly distributed numerous immunopositive cells. NCL low dose treated tissues displayed infrequent distribution of fibronectin positive cells, whereas high dose showed normalized expression with very scarcely distributed fibronectin immunpositive cells in lung tissue sections. Consequently, we examined the expression of phosphorylated Smad in lung tissue lysates. Phosphorylated Smad was highly expressed in BLM insulted tissues which was significantly diminished its levels in NCL treated tissues in dose dependent fashion. Here, expression of Smad was approximately similar in all the experimental groups. Additionally, protein expression of survivin, PDGF-BB receptor were also investigated as these proteins crucially contribute to progression of fibrosis. Considerable increase in expression of survivin and phosphorylated PDGF-BB receptor was noted in BLM treated mice. Upon treatment with NCL, these proteins were significantly reduced in both the treatment groups dose dependently. All the results of this section convey that NCL has significant inhibitory effects on fibrotic signaling (Fig. 4).

3.4. NCL reforms lung architecture and inhibits collagen accumulation in vitro and in vivo

Having adequately confirmed NCL effects of EMT and fibrotic proteins, we subsequently aimed at investigating the effect of NCL on collagen accumulation. First, immunoblotting for major collagen COL 3A1 was performed in HFL1 whole cell lysates. TGF-β1 stimulated HFL1 cells showed extremely high expression of COL 3A1 which was significantly down regulated by NCL. Similarly, western blotting of BLM treated lung homogenates also showed elevated expression of COL 1A2 and COL 3A1. In agreement with the results of *in vitro*, NCL was able to hamper the over expressed COL 1A2 and COL 3A1 dose dependently.

Further evidence for the impeding effect of NCL on collagen deposition was obtained by biochemically estimating collagen content through quantification of hydroxyproline (HP) levels in lung tissue homogenates. HP was exceptionally high in homogenates of lung tissues obtained from BLM instilled mice as compared to that of normal control mice. Reduction in collagen accumulation upon treatment with NCL was reflected as reduced HP content in lung homogenates from NCL treated mice at both dose levels. Picrosirius red staining was performed to histologically locate regions of collagen deposition in lung tissue sections of all experimental groups. BLM insulted lung sections showed numerous regions of collagen deposition displayed as red-stained tightly packed collagen fibres. NCL treated lung tissue sections showed less dense collagen fibres as compared to the BLM instilled tissues sections. The reduction in collagen accumulation was dose dependent. Next, we examined histological changes in lung after BLM instillation and the ability of NCL to restore lung framework. As depicted in Fig. 5 BLM instillation lead to disrupted lung morphology and loss of the alveolar capillary structure which was evident from collapsed alveoli and severe alveolar septal thickening when compared to normal control lung tissues. NCL treatment at both the doses restored lung architecture by significantly reducing the thickness of alveolar septa and lessening degree of fibrosis.

3.5. Effect of NCL on fibrosis associated WNT/β-catenin signaling

WNT/β-catenin signaling pathway, being one of the prime pathways contributing to fibrogenesis, effect of NCL on proteins of this pathway was evaluated both *in vitro* and *in vivo*. Western blotting of whole cell lysates was performed which revealed that TGF-β1 stimulated cells had overexpression of WNT as well as its down stream

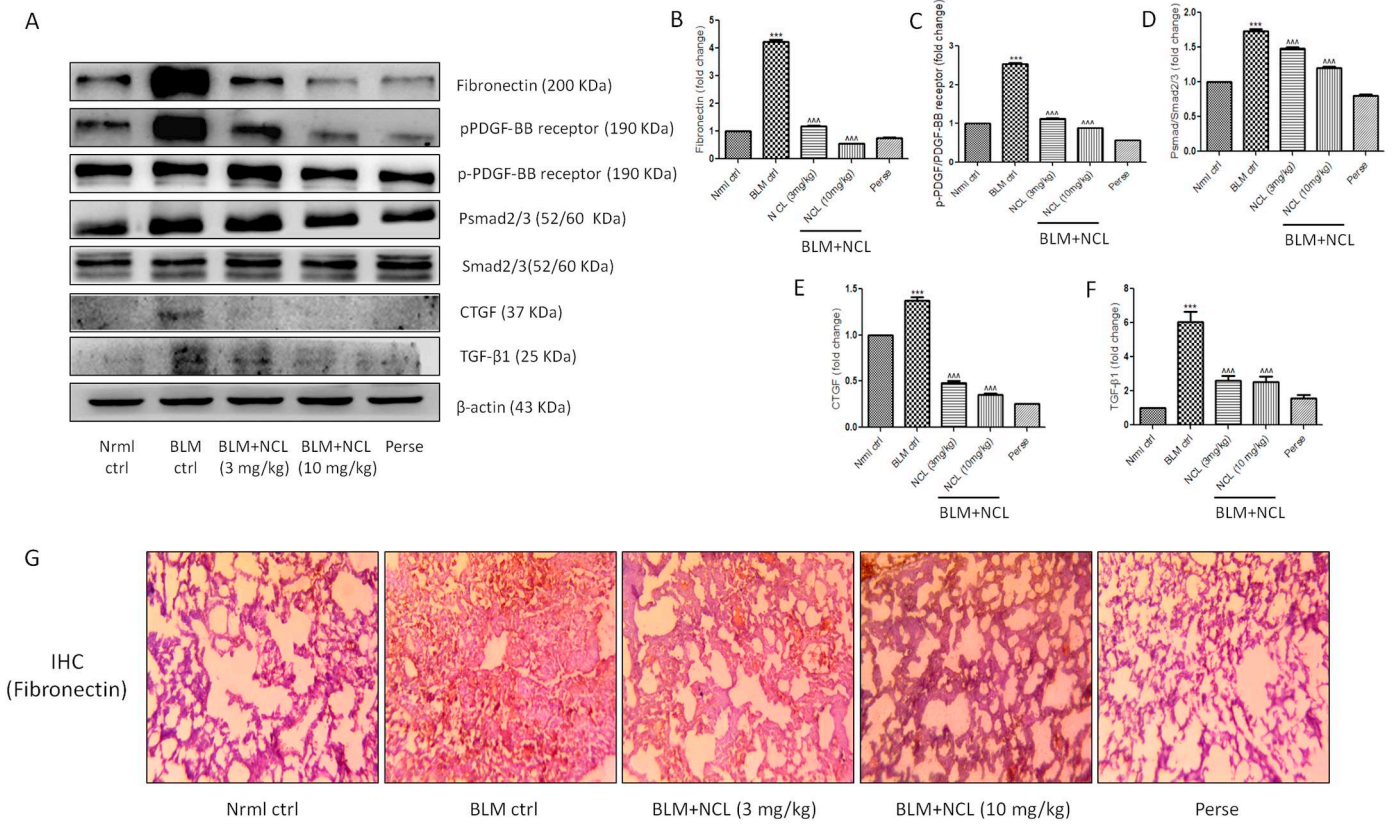

Fig. 4. NCL intervenes TGF-β/Smad signaling and down regulates expression of fibrotic markers *in vivo*. (A) Representative immuoblots of fibrotic proteins attenuated by NCL in BLM challenged mice. Densitometric analysis of quantified proteins (B) Fibronectin (C) pPDGF/PDGF-BB receptor (D) pSmad/Smad2/3 (E) CTGF (F) TGF-β1 (G) Immunohistochemical analysis for expression of fibronectin in lung tissue sections demonstrating reduced immunopositivity in NCL treated lungs (Magnification 20×). β-actin was used as internal standard for all the proteins while phosphorylated forms of proteins (pSmad & pPDGF-BB) were normalized with their respective total proteins. Data expressed as mean ± SEM, ***$p < 0.001$ of BLM *vs*. Nrml ctrl and ^^^$p < 0.001$ of NCL *vs*. BLM.

signaling molecules β-catenin, MET, CD 44, c-Myc, LEF and GSK3β. Treatment with NCL significantly down regulated all these major proteins pertaining to WNT/β-catenin signaling pathway (Fig. 6).

In lungs, a similar pattern of results was observed. BLM instilled lungs showed abnormally high levels of WNT, CD 44, c-Myc, c-Jun, LEF and GSK3β. NCL significantly attenuated the expression of the above mentioned WNT signaling proteins in a dose dependent manner. Further confirmation regarding inhibitory effect of NCL on WNT/β-catenin signaling was demonstrated by performing immunohistochemistry for evaluating the levels of β-catenin. In agreement with the results of *in vitro* study, we noted increase in immunopositivity of β-catenin in BLM challenged lung sections where as NCL treated lungs showed a significant attenuation of β-catenin positive signals (Fig. 7).

3.6. Effect of NCL on inflammation in vivo

Eventually, we investigated the effect of NCL on inflammatory proteins and cytokines by various protein expression techniques. We performed ELISA to evaluate the expression of inflammatory cytokines like TNF-α, IL-1β and IL-6 in lung tissue supernatants of all experimental groups. Lung tissues obtained from BLM challenged mice exhibited high levels of TNF-α, IL-6 and IL-1β. NCL intervention lead to attenuation of these cytokine levels at both the doses except for IL-1β where only high dose of NCL decreased the over expressed levels. Further, western blotting of TNF-α and phosphorylated form of NF-κβ was performed. Similar results were obtained *via* western blot where a dramatic increase in expression of TNF-α and p NF-κβ was noted. Treatment with NCL reduced the expression of these inflammatory proteins in a dose dependent manner. These results briefly demonstrate the anti-inflammatory potential of NCL. Moreover, staining lung tissue sections with toluidine blue showed highly distributed inflammatory cells in BLM instilled mice lungs, whereas dose dependent decrease in influx of inflammatory cells was evident in lung sections treated with NCL. Additionally, we also assessed the levels of nitric oxide in lung tissue homogenates. The results revealed that nitric oxide levels were largely elevated in BLM treated groups. Dose dependent reduction in nitric oxide levels occurred upon treatment with NCL (Fig. 8).

4. Discussion

Pulmonary fibrosis (PF) is a neoproliferative interstitial pulmonary disorder which can best described as a disorder causing destruction of lung parenchyma consequently limiting respiratory function which presents as stiffness of the lung followed by decrease in total lung capacity and increase in resistance [29,30]. Existing therapies for PF are limited to slowing disease progression which makes development of novel pharmacological interventions a compelling need [31]. Niclosamide (NCL) is a nitrosalicylanilide initially introduced as anticestodal drug in 1960s' [32,33]. Multiple researchers have made tremendous efforts to delineate the mechanism of action and targets of NCL. It is now a well established fact that NCL is a multifunctional drug which bears the ability to regulate various crucial pathways of cell signaling [34].

Drug repurposing is an attractive approach for development of pharmacological interventions for many disorders [35]. Of late, drug repurposing has gained gripping attention owing to its multiple advantages over the tedious and expensive drug developmental process of a new drug entity. Drug repositioning is a pragmatic process which has many benefits over *de novo* drug development like ready availability of

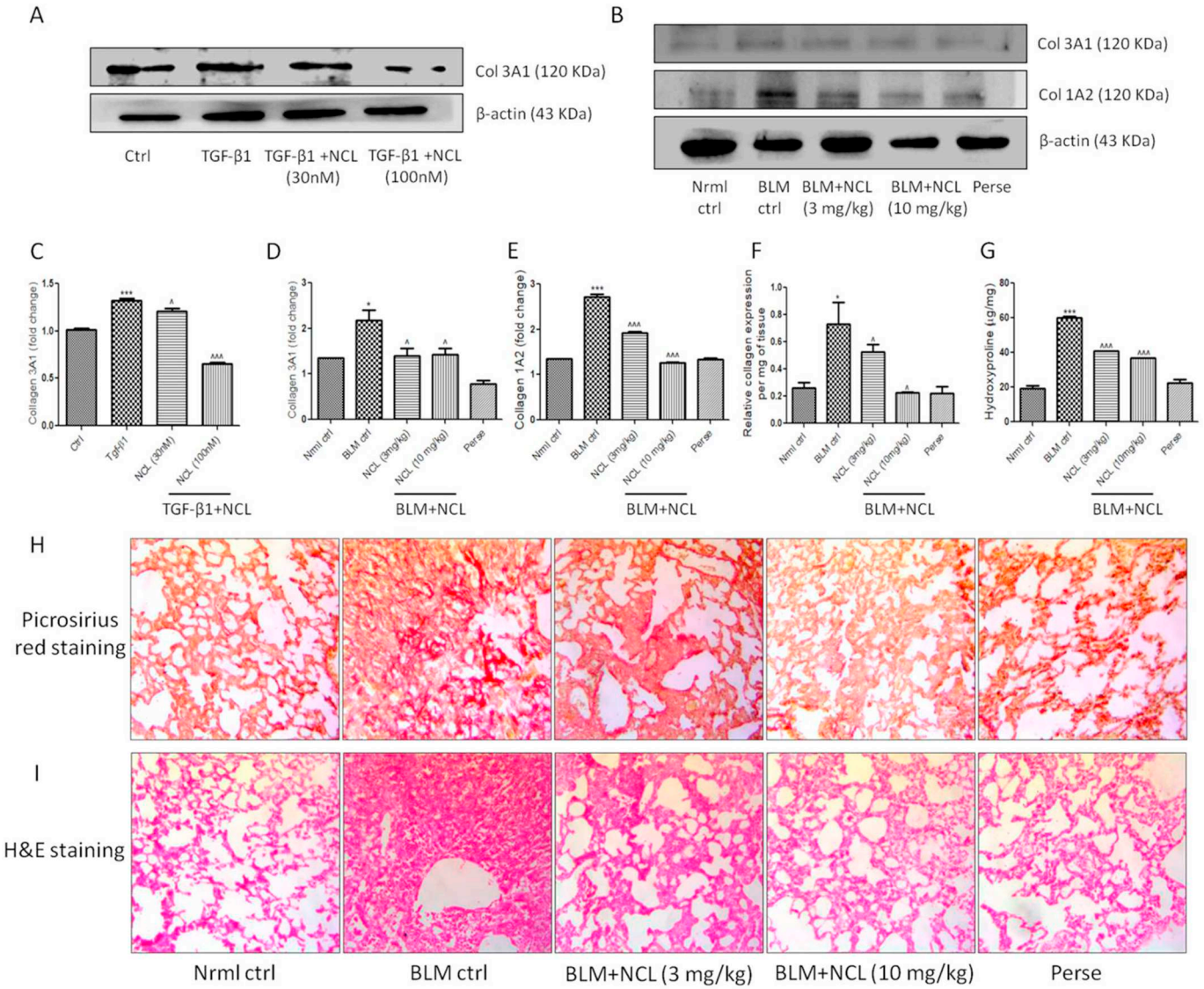

Fig. 5. Inhibitory effect of NCL on collagen accumulation both TGF-β1 stimulated HFL1 cells *in vitro* and BLM instilled mice *in vivo*. (A) Representative immunoblot of COL 3A1 in HFL1 cell lysates (B) Western blotting analysis of collagen subtypes COL 3A1 and COL 1A2 in BLM instilled mice (C) Graphical representation of quantified protein expression of COL 3A1 *in vitro*. (D & E) Densitometric analysis of immunoblots of COL 3A1 and COL 1A2 *in vivo*. (F) Relative collagen levels in lung tissues of all experimental groups as quantified by Sircol assay. Data expressed at relative collagen level per mg of protein (relative absorbance) (G) Collagen levels in lung tissues of all experimental groups as measured by hydroxyproline assay. Data expressed as µg/mg of protein. Microphotographs of lung tissue sections of all experimental groups stained with (H) Picosirius red showing the extent of collagen accumulation and (I) H&E staining demonstrating restoration of lung architecture upon treatment of NCL (Magnification 20×). Data expressed as mean ± SEM, ***$p < 0.001$, *$p < 0.05$ of disease *vs.* Nrml ctrl; ^^$p < 0.001$ and ^$p < 0.05$ of NCL *vs.* disease. (For interpretation of the references to colour in this figure legend, the reader is referred to the web version of this article.)

pharmacodynamic, pharmacokinetic, toxicity and toxicokinetic data. It is a substantial cost efficient and time effective approach in discovering new therapeutic potential for old drugs [36]. Our current study is inspired by the many success stories of drug repositioning and captivating molecular properties of NCL. Based on results provided by quite a few reports of NCL being a potential anti-fibrotic [10,20,21] this study was designed to investigate the effect of NCL in experimental model of PF both TGF-β1 induced PF *in vitro* and BLM induced *in vivo* by inhibiting WNT/β-catenin pathway. Human recombinant TGF-β1 and BLM were used as experimental inducers of PF in the current study.

Firstly, we investigated the effect of NCL on proliferation of human fibroblast cells *i.e.*; HFL1 cells. As literature findings suggest enhanced migration of fibroblasts derived from lungs with fibrotic lesions [37], we assessed the potential of NCL to curb the ability of fibroblasts to undergo migration which indicates the transdifferentiation of fibroblasts with epithelial phenotype to myofibroblasts of mesenchymal phenotype. NCL demonstrated potential capacity to inhibit proliferation and migration of human fibroblasts as evident from relative occupancy of denuded area in wound scratch assay (Fig. 2). Concept of EMT, initially defined in the context of embryonic development [38], has been established to be notorious for pathological contribution to fibrosis [39]. EMT process initiated by various factors, TGF-β1 being one of them, is characterized by functional transition of fibroblasts (epithelial cells) to motile myofibroblasts (mesenchymal cells) [40]. These changes are associated with loss of epithelial proteins E-cadherin and a corresponding up regulation of mesenchymal proteins like N-cadherin and α-SMA, which give myofibroblasts ability to gain contractility [41]. EMT changes induced by human recombinant TGF-β1 *in vitro* and BLM *in vivo* were regulated significantly by NCL. NCL restored the protein expression of E-cadherin while down regulated the expression of α-SMA expression both *in vitro* and *in vivo*. Besides, protein expression of N-cadherin was inhibited *in vivo* by NCL, which

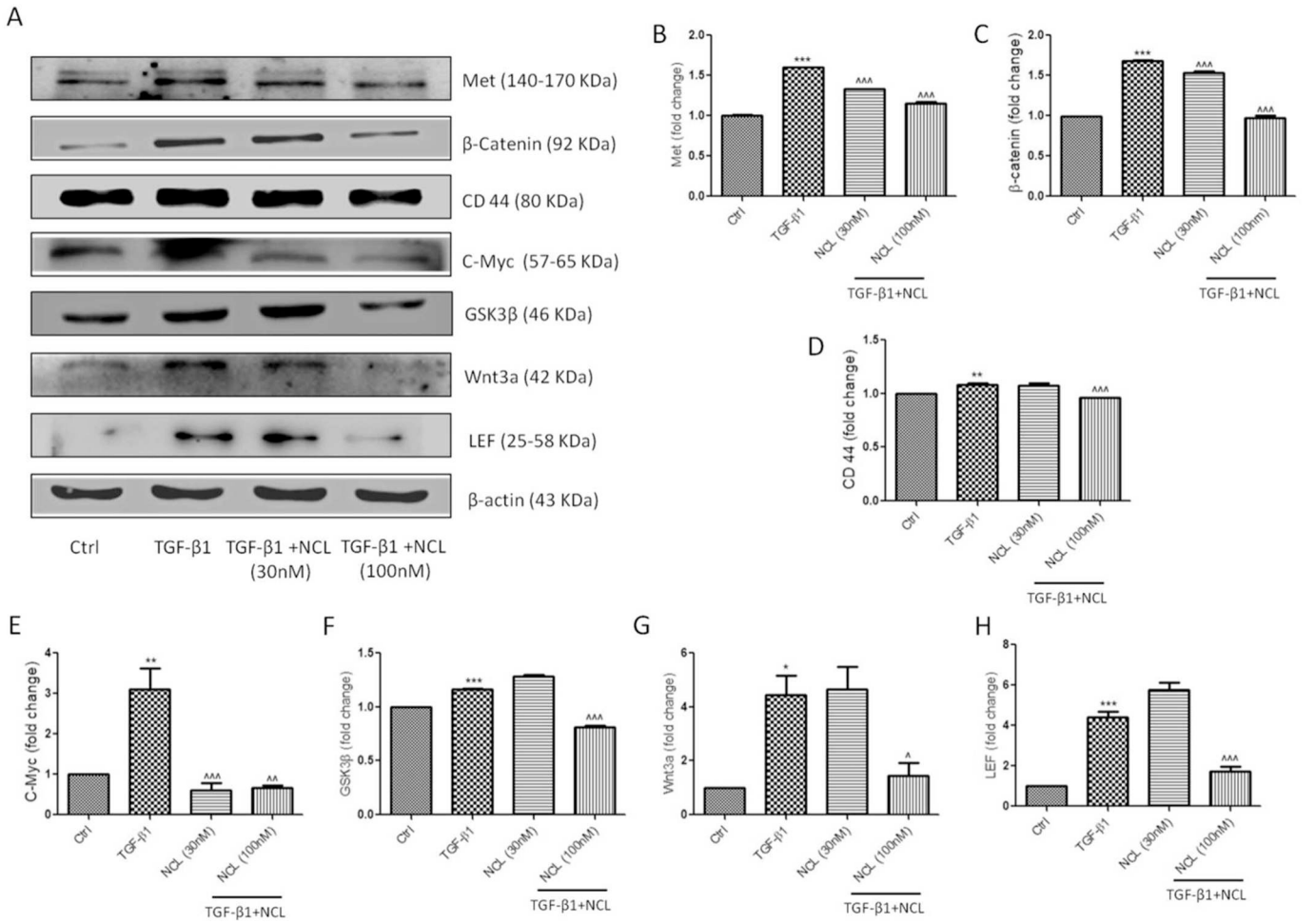

Fig. 6. Attenuation of WNT/β-catenin signaling pathway by NCL in TGF-β1 treated HFL1 cells. (A) Immuno blotting analysis of proteins belonging to WNT/β-catenin signaling pathway. Graphical representation of quantified protein expression of (B) Met (C) β-catenin (D) CD 44 (E) C-Myc (F) GSK3β (G) WNT3a (H) LEF. Data expressed as mean ± SEM $***p < 0.001$ $**p < 0.01$, $*p < 0.05$ of TGF-β1 *vs*. Nrml ctrl; $\hat{}\hat{}\hat{}p < 0.001$ $\hat{}\hat{}p < 0.01$ and $\hat{}p < 0.05$ of NCL *vs*. TGF-β1.

demonstrates the ability of NCL to adequately amends disrupted EMT proteins (Fig. 2).

Canonical Smad dependent TGF-β1 signaling cascade is the prime signaling pathway and the major driver of fibrosis. Ligands binding to specific TGF-β1 receptors activate the TGF-β/Smad axis which results in phosphorylation and translocation of Smad2/3 to the nucleus to execute signals of fibrotic gene transcription [42]. Thus, we evaluated the effect of NCL on TGF-β/Smad signaling axis and the expression of proteins involved in fibrotic signaling both *in vitro* and *in vivo*. NCL down regulated the expression of major fibrotic proteins TGF-β1, CTGF, phosphorylated Smad2/3 and fibronectin in TGF-β1 stimulated HFL1 cells as apparent from immunoblotting studies (Fig. 3). Consistent with the *in vitro* results, these fibrotic proteins were significantly suppressed by NCL *in vivo* in experimental model of BLM induced PF, as evident from western blots of the same. Further, significant reduction in the immunosignal of fibronectin as observed from immunohistochemistry strengthened the evidence of NCL being an anti-fibrotic agent (Fig. 4).

PDGFs and their receptors have been extensively studied for their role in cell proliferation, differentiation, migration and tissue remodeling [43]. Existing literature supports PDGF subtype BB to be a stronger mitogen and chemoattractant for fibroblasts than the other PDGF subtypes [44,45]. This is backed by the fact that fibroblasts derived from idiopathic pulmonary fibrosis patients demonstrated marked increase in PDGF-BB receptor expression compared to the controls [46]. Prominent decrease in expression of phosphorylated form of PDGF-BB receptor was noted upon treatment with NCL, as evident from immunoblotting studies (Fig. 4).

TGF-β1 is a well known stimulator of collagen synthesis and accumulation [47] in the lung by regulation of collagen turnover through myofibroblasts which synthesize excess collagen as compared to their fibroblasts counterparts leading to disruption of lung architecture [48]. Maximal restoration of lung architecture, frame work and alveolar thickness was noted upon treatment with NCL. Additionally, NCL also significantly hindered the accumulation of collagen which was evident microscopically through picro sirius red tissue staining. These results coincided with biochemically quantified collagen by Hydroxyproline levels and Sircol assay. Parallely, *in vitro* and *in vivo* immunoblotting showed sharp reduction in expression of collagen subtypes COL 1A2 and COL 3A1 by NCL. These findings in our study implicate that NCL strongly prevents abnormal accumulation of collagen both *in vitro* and *in vivo* (Fig. 5).

Evidences from existing literature are strong enough to demonstrate beyond doubt the aberrant activation of Wingless/Int (WNT)/β-catenin signaling associated with downregulation of endogenous WNT antagonists in PF [49,50]. First report of WNT and it effector β-catenin involvement in fibrogenesis was established several years ago, since then various studies have proven the pathogenic role of this signaling cascade in development of PF [51–53]. Additionally, nuclear accumulation of β-catenin is known to induce the process of EMT in fibroblasts [50]. NCL is an established inhibitor of WNT/β-catenin and their downstream molecules [22]. In agreement with the literature with respect to inhibiting properties of NCL, we observed significant

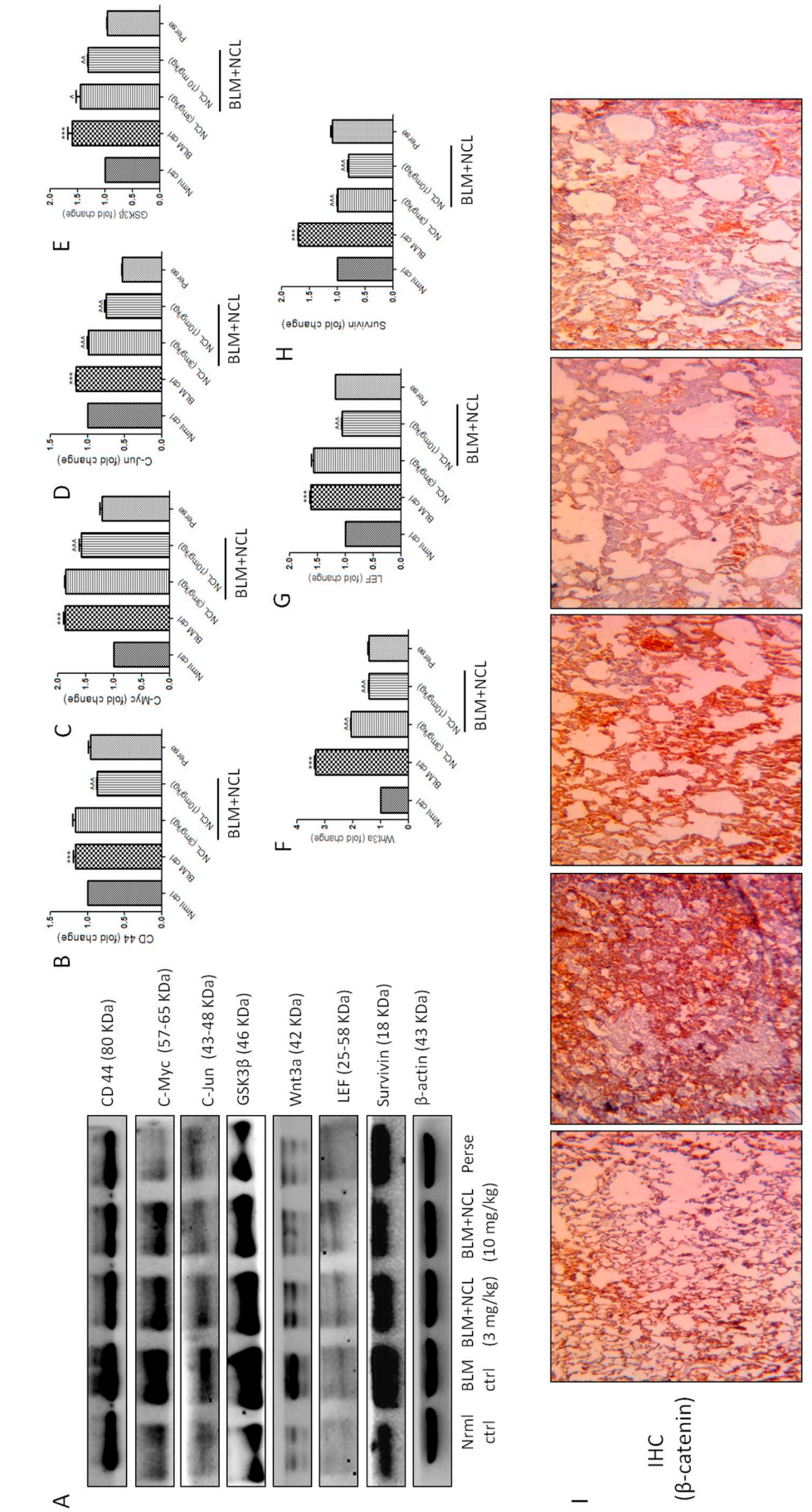

Fig. 7. Effect of NCL on regulation of WNT/β-catenin signaling *in vivo*. (A) Representative immunoblots of proteins involved in WNT/β-catenin signaling. Densitometric analysis of (B) CD 44 (C) C-Myc (D) C-Jun (E) GSK3β (F) WNT3a (G) LEF (H) Survivin. Data expressed as mean ± SEM, $***p < 0.001$ of BLM *vs.* Nrml ctrl; $^{\wedge\wedge\wedge}p < 0.001$, $^{\wedge}p < 0.01$ and $p < 0.05$ of NCL *vs.* BLM. (I) Representative microphotographs of lung tissue sections immunostained with β-catenin antibody as analyzed by immunohistochemistry demonstrating the decreased immunopositivity of β-catenin in NCL treated lung tissue sections (Magnification 20×).

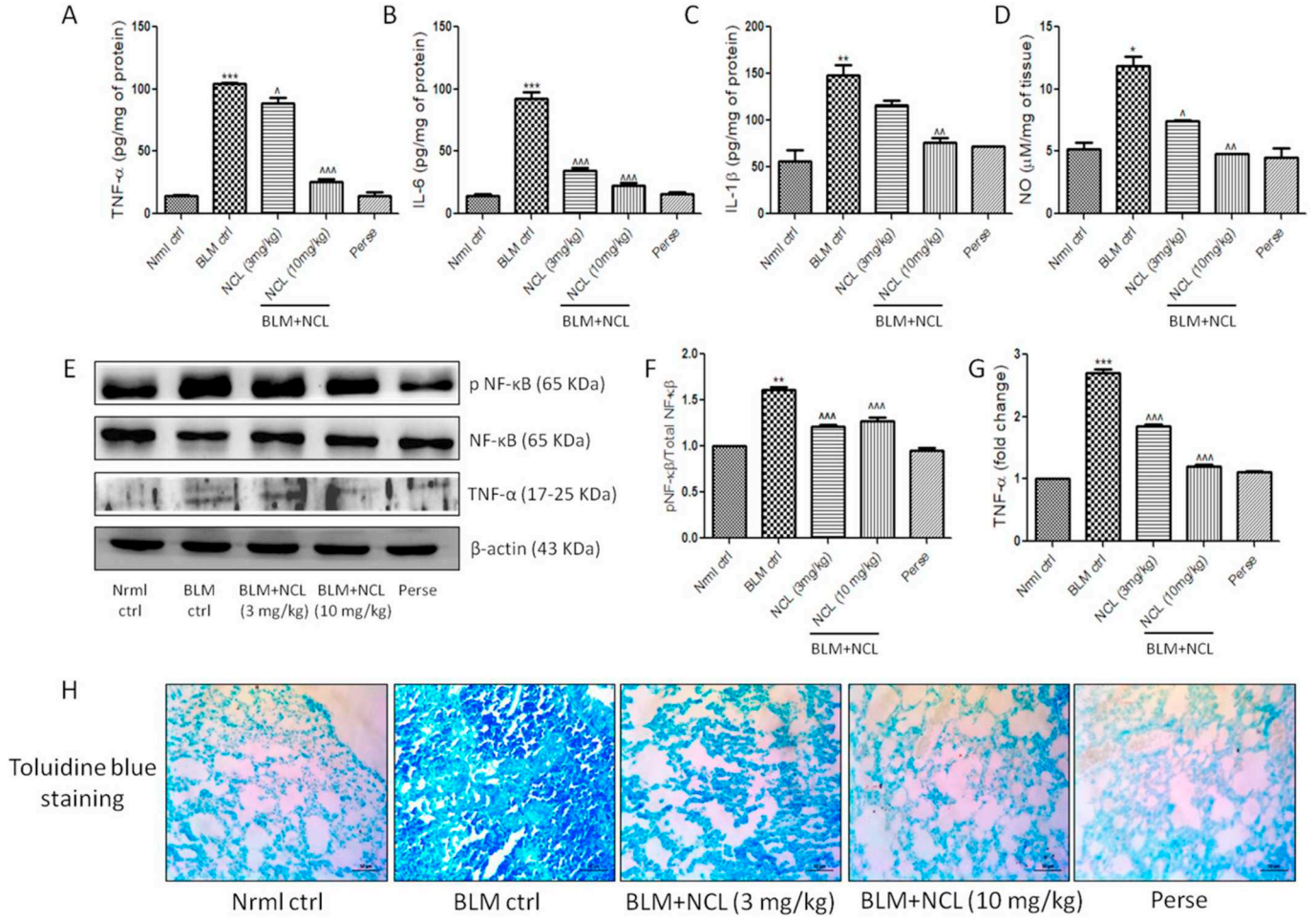

Fig. 8. Effect of NCL of inflammatory proteins in BLM challenged lungs. Quantification of expression of inflammatory cytokines (A) TNF-α (B) IL-6 and (C) IL-1β by ELISA. (D) Estimation of NO levels (E) Representative western blots of inflammatory proteins in lung tissue lysates (F & G) Graphical representation of pNF-κβ/NF-κβ and TNF-α respectively. β-actin was used as internal standard for TNF-α while NF-κβ was normalized with its respective total proteins.$^{***}p < 0.001$, $^{**}p < 0.01$ and $^{*}p < 0.05$ of BLM *vs*. Nrml ctrl; $^{\wedge\wedge\wedge}p < 0.001$, $^{\wedge\wedge}p < 0.01$, $^{\wedge}p < 0.05$ of NCL *vs*. BLM. (H) Microphotographs of lung tissue sections of all experimental groups stained with toluidine blue for assessment of extent of inflammatory cell influx.

alleviation in the expression of WNT, nuclear accumulation of β-catenin, along with the downstream proteins of this pathway such as Met, CD44, C-Myc and LEF in whole cell lysates of TGF-β1 stimulated NCL treated HFL1 cells *in vitro* (Fig. 6). Similarly, WNT, CD44, C-Myc, C-Jun and LEF were sharply decreased upon treated with NCL as observed from western blotting of lung tissue samples of all the experimental groups. Substantiating this evidence, immunohistochemistry of β-catenin demonstrated diminished nuclear retention in lung tissue sections treated with NCL. Survivin is the smallest member of Inhibitor of Apoptosis (IAP) family, which beholds the critical function of cell cycle progression [54,55]. Thus, robust expression of survivin is not surprising and is also well studied, which represents the apoptosis resistant phenotype of fibroblasts. NCL significantly attenuated the expression of survivin in both *in vitro* and *in vivo* experimental models. Further, GSK3β which is a serine/threonine protein kinase, which promotes fibrogenic activity as a partaker in execution of WNT/β-catenin pathway [56,57], was also prominently attenuated by NCL (Fig. 7).

As PF is an inflammation driven fibrotic process [58], attenuating the expression of inflammatory proteins and cytokines would therefore significantly contribute in alleviation of PF. In the current study, NCL treatment to BLM challenged mice demonstrated reduced levels of pro-inflammatory cytokines IL-6, IL-1β and TNF-α as evident from ELISA. Additionally we also found that upon NCL treatment, there was significant reduction in levels of nitric oxide which is a pro-inflammatory mediator in pathogenesis of fibrosis [59]. Toluidine blue staining of lung tissue sections showed reduced inflammatory cell influx in NCL treated lung tissue sections (Fig. 8). Anti-inflammatory activity of NCL was further justified by BAL fluid analysis which showed reduced count of differential inflammatory cells (Fig. 1). All the above discussed findings of this study demonstrate the anti-fibrotic potential of NCL in ameliorating PF progression.

5. Conclusion

Concluding the current study, it can be said that NCL demonstrates strong anti-fibrotic potential by attenuating and regulating fibroblast migration, EMT process, ECM deposition, TGF-β/Smad signaling, WNT/β-catenin pathway and inflammation. Further, considering the results of our study in addition to established *in silico* data, repurposing of NCL as an anti-fibrotic agent would be cost effective as well as a promising approach to treat pulmonary fibrosis.

Conflict of interest

The authors declare no conflict of interest.

Funding

This study was supported financially by the Department of Pharmaceuticals, Ministry of Chemicals and Fertilizers, Government of

India. The authors would like to thank the Department of Biotechnology (DBT), Govt. of India, for the financial support to Dr. Chandraiah Godugu *via* a North East-Twinning Grant: MAP/2015/58, an Indo-Brazil Grant: DBT/IC-2/Indo-Brazil/2016-19/01 and a DST-Science and Engineering Board-Early Career Research Award (SERB-ECR) Grant: ECR/2016/000007.

Authors contributions

RB and GP contributed equally to this work. CG, RB and GP designed the research work. CG, RB, GP and SB performed the research. RB, GP, SB and CG wrote the manuscript. All authors reviewed the final version of the manuscript.

Acknowledgements

The authors acknowledge Department of Pharmaceuticals, Ministry of Chemicals and Fertilizers, Government of India.

References

[1] S.M. Corsello, J.A. Bittker, Z. Liu, J. Gould, P. McCarren, J.E. Hirschman, et al., The drug repurposing hub: a next-generation drug library and information resource, Nat. Med. 23 (4) (2017) 405.
[2] T.-W. Kim, Drug repositioning approaches for the discovery of new therapeutics for Alzheimer's disease, Neurotherapeutics 12 (1) (2015) 132–142.
[3] M.D. Reed, The Rescue and Repurposing of Pharmaceuticals: Augmenting the Drug Development Paradigm, Pediatric Pharmacy Advocacy Group, 2016.
[4] G. Jin, S.T. Wong, Toward better drug repositioning: prioritizing and integrating existing methods into efficient pipelines, Drug Discov. Today 19 (5) (2014) 637–644.
[5] A. Nagaraj, Q. Wang, P. Joseph, C. Zheng, Y. Chen, O. Kovalenko, et al., Using a novel computational drug-repositioning approach (DrugPredict) to rapidly identify potent drug candidates for cancer treatment, Oncogene 37 (3) (2018) 403.
[6] M. Zhang, G. Schmitt-Ulms, C. Sato, Z. Xi, Y. Zhang, Y. Zhou, et al., Drug repositioning for Alzheimer's disease based on systematic 'omics' data mining, PLoS One 11 (12) (2016) e0168812.
[7] Y. Chen, C. Murillo-Solano, M.G. Kirkpatrick, T. Antoshchenko, H.-W. Park, J.C. Pizarro, Repurposing drugs to target the malaria parasite unfolding protein response, Sci. Rep. 8 (1) (2018) 10333.
[8] K.T. Andrews, G. Fisher, T.S. Skinner-Adams, Drug repurposing and human parasitic protozoan diseases, Int. J. Parasitol. Drugs Drug Resist. 4 (2) (2014) 95–111.
[9] E. March-Vila, L. Pinzi, N. Sturm, A. Tinivella, O. Engkvist, H. Chen, et al., On the integration of in silico drug design methods for drug repurposing, Front. Pharmacol. 8 (2017) 298.
[10] E. Karatzas, M. Bourdakou, G. Kolios, G. Spyrou, Drug repurposing in idiopathic pulmonary fibrosis filtered by a bioinformatics-derived composite score, Sci. Rep. 7 (1) (2017) 12569.
[11] A. Tzouvelekis, V. Tzilas, M. Dassiou, D. Bouros, Metformin in idiopathic pulmonary fibrosis "seeking the holy-grail through drug-repositioning", Respiration (2018) 1–3.
[12] S. Garantziotis, M.P. Steele, D.A. Schwartz, Pulmonary fibrosis: thinking outside of the lung, J. Clin. Invest. 114 (3) (2004) 319–321.
[13] A. Biernacka, M. Dobaczewski, N.G. Frangogiannis, TGF-β signaling in fibrosis, Growth Factors 29 (5) (2011) 196–202.
[14] Y. Guo, L. Xiao, L. Sun, F. Liu, Wnt/β-catenin signaling: a promising new target for fibrosis diseases, Physiol. Res. 61 (4) (2012).
[15] O. Burgy, M. Königshoff, The WNT signaling pathways in wound healing and fibrosis, Matrix Biol. 68–69 (2018) 67–80.
[16] B.C. Willis, J.M. Liebler, K. Luby-Phelps, A.G. Nicholson, E.D. Crandall, R.M. du Bois, et al., Induction of epithelial-mesenchymal transition in alveolar epithelial cells by transforming growth factor-β1: potential role in idiopathic pulmonary fibrosis, Am. J. Pathol. 166 (5) (2005) 1321–1332.
[17] N. Sakai, A.M. Tager, Fibrosis of two: epithelial cell-fibroblast interactions in pulmonary fibrosis, Biochim. Biophys. Acta (BBA) - Mol. Basis Dis. 1832 (7) (2013) 911–921.
[18] W. Chen, R.A. Mook Jr., R.T. Premont, J. Wang, Niclosamide: beyond an antihelminthic drug, Cell. Signal. 41 (2017) 89–96.
[19] J.-X. Pan, K. Ding, C.-Y. Wang, Niclosamide, an old antihelminthic agent, demonstrates antitumor activity by blocking multiple signaling pathways of cancer stem cells, Chin. J. Cancer 31 (4) (2012) 178–184.
[20] F. Morin, N. Kavian, C. Nicco, O. Cerles, C. Chéreau, F. Batteux, Niclosamide prevents systemic sclerosis in a reactive oxygen species–induced mouse model, J. Immunol. (2016) 1502482.
[21] X. Chang, X. Zhen, J. Liu, X. Ren, Z. Hu, Z. Zhou, et al., The antihelmenthic phosphate niclosamide impedes renal fibrosis by inhibiting homeodomain-interacting protein kinase 2 expression, Kidney Int. 92 (3) (2017) 612–624.
[22] R.C. Arend, A.I. Londoño-Joshi, A. Gangrade, A.A. Katre, C. Kurpad, Y. Li, et al., Niclosamide and its analogs are potent inhibitors of Wnt/β-catenin, mTOR and STAT3 signaling in ovarian cancer, Oncotarget 7 (52) (2016) 86803.
[23] M. Chen, J. Wang, J. Lu, M.C. Bond, X.-R. Ren, H.K. Lyerly, et al., The anti-helminthic niclosamide inhibits Wnt/Frizzled1 signaling, Biochemistry 48 (43) (2009) 10267–10274.
[24] V. Pooladanda, S. Bandi, S.R. Mondi, K.M. Gottumukkala, C. Godugu, Nimbolide epigenetically regulates autophagy and apoptosis in breast cancer, Toxicol. in Vitro 51 (2018) 114–128.
[25] S. Bale, P. Venkatesh, M. Sunkoju, C. Godugu, An adaptogen: withaferin a ameliorates in vitro and in vivo pulmonary fibrosis by modulating the interplay of fibrotic, matricelluar proteins, and cytokines, Front. Pharmacol. 9 (2018) 248.
[26] A. Khurana, S. Tekula, C. Godugu, Nanoceria suppresses multiple low doses of streptozotocin-induced type 1 diabetes by inhibition of Nrf2/NF-κB pathway and reduction of apoptosis, Nanomedicine 13 (15) (2018).
[27] S. Bale, M. Sunkoju, S.S. Reddy, V. Swamy, C. Godugu, Oropharyngeal aspiration of bleomycin: an alternative experimental model of pulmonary fibrosis developed in Swiss mice, Indian J. Pharmacol. 48 (6) (2016) 643.
[28] C. Godugu, A.R. Patel, R. Doddapaneni, J. Somagoni, M. Singh, Approaches to improve the oral bioavailability and effects of novel anticancer drugs berberine and betulinic acid, PLoS One 9 (3) (2014) e89919.
[29] C. Vancheri, Idiopathic pulmonary fibrosis: an altered fibroblast proliferation linked to cancer biology, Proc. Am. Thorac. Soc. 9 (3) (2012) 153–157.
[30] A. Cortes-Telles, L. Forkert, D.E. O'Donnell, O. Morán-Mendoza, Idiopathic pulmonary fibrosis: new insights to functional characteristics at diagnosis, Can. Respir. J. 21 (3) (2014) e55–e60.
[31] K.C. Meyer, C.A. Decker, Role of pirfenidone in the management of pulmonary fibrosis, Ther. Clin. Risk Manag. 13 (2017) 427.
[32] J. Zhou, B. Jin, Y. Jin, Y. Liu, J. Pan, The antihelminthic drug niclosamide effectively inhibits the malignant phenotypes of uveal melanoma in vitro and in vivo, Theranostics 7 (6) (2017) 1447.
[33] G. Panic, U. Duthaler, B. Speich, J. Keiser, Repurposing drugs for the treatment and control of helminth infections, Int. J. Parasitol. Drugs Drug Resist. 4 (3) (2014) 185–200.
[34] J. Natera, E. Gatica, C. Challier, D. Possetto, W. Massad, S. Miskoski, et al., On the photooxidation of the multifunctional drug niclosamide. A kinetic study in the presence of vitamin B2 and visible light, Redox Rep. 20 (6) (2015) 259–266.
[35] T.T. Ashburn, K.B. Thor, Drug repositioning: identifying and developing new uses for existing drugs, Nat. Rev. Drug Discov. 3 (8) (2004) 673.
[36] S. Kato, S.L. Moulder, N.T. Ueno, J.J. Wheler, F. Meric-Bernstam, R. Kurzrock, et al., Challenges and perspective of drug repurposing strategies in early phase clinical trials, Oncoscience 2 (6) (2015) 576.
[37] H. Suganuma, A. Sato, R. Tamura, K. Chida, Enhanced migration of fibroblasts derived from lungs with fibrotic lesions, Thorax 50 (9) (1995) 984–989.
[38] R. Kalluri, R.A. Weinberg, The basics of epithelial-mesenchymal transition, J. Clin. Invest. 119 (6) (2009) 1420–1428.
[39] R. Kalluri, E.G. Neilson, Epithelial-mesenchymal transition and its implications for fibrosis, J. Clin. Invest. 112 (12) (2003) 1776–1784.
[40] M.K. Wendt, T.M. Allington, W.P. Schiemann, Mechanisms of the epithelial–mesenchymal transition by TGF-β, Future Oncol. 5 (8) (2009) 1145–1168.
[41] S. Lamouille, J. Xu, R. Derynck, Molecular mechanisms of epithelial–mesenchymal transition, Nat. Rev. Mol. Cell Biol. 15 (3) (2014) 178.
[42] X. Yue, B. Shan, J.A. Lasky, TGF-β: titan of lung fibrogenesis, Curr. Enzym. Inhib. 6 (2) (2010) 67–77.
[43] N. Noskovičová, M. Petřek, O. Eickelberg, K. Heinzelmann, Platelet-derived growth factor signaling in the lung. From lung development and disease to clinical studies, Am. J. Respir. Cell Mol. Biol. 52 (3) (2015) 263–284.
[44] Y. Aono, M. Kishi, Y. Yokota, M. Azuma, K. Kinoshita, A. Takezaki, et al., Role of platelet-derived growth factor/platelet-derived growth factor receptor axis in the trafficking of circulating fibrocytes in pulmonary fibrosis, Am. J. Respir. Cell Mol. Biol. 51 (6) (2014) 793–801.
[45] Y. Li, H.-t. Ren, Endostatin inhibits fibrosis by modulating the PDGFR/ERK signal pathway: an in vitro study, J Zhejiang Univ Sci B 18 (11) (2017) 994–1001.
[46] K.E. Hostettler, J. Zhong, E. Papakonstantinou, G. Karakiulakis, M. Tamm, P. Seidel, et al., Anti-fibrotic effects of nintedanib in lung fibroblasts derived from patients with idiopathic pulmonary fibrosis, Respir. Res. 15 (1) (2014) 157.
[47] E.F. Johnston, T.E. Gillis, Transforming growth factor beta-1 (TGF-β1) stimulates collagen synthesis in cultured rainbow trout cardiac fibroblasts, J. Exp. Biol. 220 (2017) 2645–2653 (jeb. 160093).
[48] P.-S. Lin, H.-H. Chang, C.-Y. Yeh, M.-C. Chang, C.-P. Chan, H.-Y. Kuo, et al., Transforming growth factor beta 1 increases collagen content, and stimulates procollagen I and tissue inhibitor of metalloproteinase-1 production of dental pulp cells: role of MEK/ERK and activin receptor-like kinase-5/Smad signaling, J. Formos. Med. Assoc. 116 (5) (2017) 351–358.
[49] J. Shi, F. Li, M. Luo, J. Wei, X. Liu, Distinct roles of Wnt/β-catenin signaling in the pathogenesis of chronic obstructive pulmonary disease and idiopathic pulmonary fibrosis, Mediat. Inflamm. 2017 (2017).
[50] H. Baarsma, M. Königshoff, 'WNT-er is coming': WNT signalling in chronic lung diseases, Thorax 72 (8) (2017) 746–759.
[51] E.E. Morrisey, Wnt signaling and pulmonary fibrosis, Am. J. Pathol. 162 (5) (2003) 1393.
[52] M. Königshoff, N. Balsara, E.-M. Pfaff, M. Kramer, I. Chrobak, W. Seeger, et al., Functional Wnt signaling is increased in idiopathic pulmonary fibrosis, PLoS One 3

(5) (2008) e2142.
[53] L. Liu, B. Carron, H.T. Yee, T.-A. Yie, M. Hajjou, W.N. Rom, Wnt pathway in pulmonary fibrosis in the bleomycin mouse model, J. Environ. Pathol. Toxicol. Oncol. 28 (2) (2009).
[54] P.K. Jaiswal, A. Goel, R. Mittal, Survivin: a molecular biomarker in cancer, Indian J. Med. Res. 141 (4) (2015) 389.
[55] T.H. Sisson, T.M. Maher, I.O. Ajayi, J.E. King, P.D. Higgins, A.J. Booth, et al., Increased survivin expression contributes to apoptosis-resistance in IPF fibroblasts, Adv. Biosci. Biotechnol. 3 (6A) (2012) 657.
[56] E. Beurel, S.F. Grieco, R.S. Jope, Glycogen synthase kinase-3 (GSK3): regulation, actions, and diseases, Pharmacol. Ther. 148 (2015) 114–131.
[57] S.P. Singh, S. Tao, T.A. Fields, S. Webb, R.C. Harris, R. Rao, Glycogen synthase kinase-3 inhibition attenuates fibroblast activation and development of fibrosis following renal ischemia-reperfusion in mice, Dis. Model. Mech. 8 (8) (2015) 931–940.
[58] B.D. Bringardner, C.P. Baran, T.D. Eubank, C.B. Marsh, The role of inflammation in the pathogenesis of idiopathic pulmonary fibrosis, Antioxid. Redox Signal. 10 (2) (2008) 287–302.
[59] J. Sharma, A. Al-Omran, S. Parvathy, Role of nitric oxide in inflammatory diseases, Inflammopharmacology 15 (6) (2007) 252.